Microstructural characterization of ball-milled metal matrix nanocomposites (Cr, Ni, Ti)-25 wt. % (Al_2O_{3np}, SiC_{np})

Y. Afkham[1], R. Azari Khosroshahi [1], R. Taherzadeh Mousavian[1,*], D. Brabazon [2], R. Kheirifard [1]

1: Faculty of Materials Engineering, Sahand University of Technology, Tabriz, Iran
2: Advanced Processing Technology Research Centre, School of Mechanical & Manufacturing Engineering, Dublin City University, Dublin 9, Ireland
Email: r_taherzadeh@sut.ac.ir
Tel: +98 919 959 1160, Fax: +98 21 44412039

Abstract

The microstructure of high-temperature metals such as Ti, Ni, and Cr can be modified using ceramic nanoparticles to form metal matrix nanocomposites (MMNCs). Such materials are generally prepared via powder metallurgy routes. In this study, 25 wt. % SiC_{np} and Al_2O_{3np} were separately ball-milled as a reinforcement of Ti, Cr, and Ni matrices to investigate their effects on the phase formation and morphology of the MMNCs. The XRD, SEM, and FESEM results indicated that the alumina-metal system could not be thermodynamically stable in a high-energy ball mill, while the SiC reinforcement could be retained and milled with the metals even after 24 hours. It was further observed that the distribution of nanoparticles was not affected by the type of metal, ceramic, and milling time. Finally, it was determined that the nanoparticles significantly reduced the average particle size of composite powders.

Keywords: Ball milling; Nanoparticle; Metal matrix nanocomposite; Cr; Ti; Ni.

1. Introduction

Although metal matrix composites (MMCs) have regularly been produced and utilised in industry for a long time, there remains a strong focus on enhancing their properties and developing an understanding of the causative influences on properties (Boostani, Yazdani, et al. 2015; Boostani, Tahamtan, et al. 2015; Boostani, Mousavian, et al. 2015; Mousavian et al. 2016). It is well know that MMCs can provide economic benefits from increased specific strength components (Allison and Cole 1993; Miracle 2005; de Oliveira et al. 2015). The matrix phase in the composites in this case is a flexible metal, which is mainly chosen from super alloys, aluminum, magnesium, titanium, and copper alloys (Valibeygloo, Khosroshahi, and Mousavian 2013; Mojtaba et al. 2012; Mousavian et al. 2016; Ibrahim, Mohamed, and Lavernia 1991; Boostani et al. 2016; Bernoosi, Azari Khosroshahi, and Taherzadeh Mousavian 2014). High operation temperatures, strengths, wear resistance, and a greater resistance to corrosion are advantages of MMCs. Such materials are used in many applications in automotive, aerospace, and electrical industries (Kaczmar, Pietrzak, and Włosiński 2000). Generally, the production methods of MMCs can be classified into three categories; casting, powder metallurgy and mechanical alloying methods, each of which have their own merits and demerits (He, Han, and Jackson 2008).

Nowadays mechanical alloying has become as the most common method for manufacturing MMCs. In particular, for metals that have high melting temperatures, liquid-state methods are not economical. An additional advantage of mechanical alloying is the relative ease of this production process (Rosas et al. 2005; Suryanarayana and Al-Aqeeli 2013). This process is used to produce and mix both the metal and ceramic powders in the solid-state form (Suryanarayana, Ivanov, and Boldyrev 2001). Cold welding and fracturing are the two major phenomena in the

mechanical alloying process. The alloying procedure continues until the rate of welding and fracturing becomes balanced (Mosleh, Ehteshamzadeh, and Mousavian 2014; Mousavian et al. 2014; Zebarjad and Sajjadi 2006; Khakbiz and Akhlaghi 2009; Rivera et al. 2012; Nekouee et al. 2015; Forouzan et al. 2015; Mousavian et al. 2011; Mousavian, Sharafi, and Shariat 2011).

Recently, the introduction of nanoparticles in the matrix has been reported as a method for modification of microstructure and properties of MMCs (Casati and Vedani 2014). However, one of the negative characteristics of nanoparticles is the high tendency of their agglomeration and cluster formation. Uncontrolled agglomeration, which occurs through van der Waals forces, is a common phenomenon that increases the inhomogeneity of composite structures (Mahboob, Sajjadi, and Zebarjad 2011; Pramanik and Littlefair 2013; Mohanty et al. 2014). One method to overcome this obstacle is ball milling. This method has proved its proficiency in distributing the nanoparticles into the metal matrix in an efficient way (Gajović et al. 2001; Suryanarayana 2001). This process takes place in a sealed container by frequent collisions between rigid balls, which generate a high pressure, and the powders between the balls, which are ground into finer powders due to the cascading effect of these collisions (Ozdemir et al. 2008; Zhou et al. 2015). By using ball milling, Mobasherpour et al. (Mobasherpour, Tofigh, and Ebrahimi 2013) studied the effect of the amount of entrained nano-size Al_2O_3 reinforcement on the mechanical behavior of aluminum alloy composites. Their results revealed the uniform distribution of the nanoparticles in the matrix system. Another recent research which studied the effect of milling time on the nanoparticles dispersion, found that the uniformity of the as-milled powders was enhanced with increased milling time (Zawrah et al. 2013).

The purpose of this study was to investigate the effects of the milling time and matrix type on the distribution of the SiC_{np} and Al_2O_{3np} in the matrix phase, as well as the phase morphology and

changes of the as-milled reinforced powders. The pure metal powders were milled under similar conditions and characterised in order to have a baseline for comparison to the morphology of composite powders.

2. Material and methods

Titanium, nickel, and chromium powders were used in the present study as the metal matrices. As reinforcement, Al_2O_3 and SiC nanoparticles were separately used. The characteristics of the examined powders are presented in Table 1. The morphologies of the Ti, Cr, Ni, and as-received Al_2O_3 (all from Shanghai Dinghan, China) and SiC (from US Research Nanomaterials, USA) nano powders are also shown in Fig. 1. As can be seen, both of the nanoparticles were in agglomerated form before ball milling with an almost spherical shape, while the titanium powders had sharp edges like ceramic materials, Ni had a fine chain-like morphology, and the Cr particles had an irregular coarse shape.

Table 1. Characteristics of the starting powders.

Powder	Average particle size	Purity (%)	Crystalline structure
Ti	<50 μm	>99	HCP
Ni	<5 μm	>99	FCC
Cr	>150 μm	>99	BCC
Al_2O_3	40 nm	99.0	α (hexagonal)
SiC	<40 nm	99.0	β (cubic)

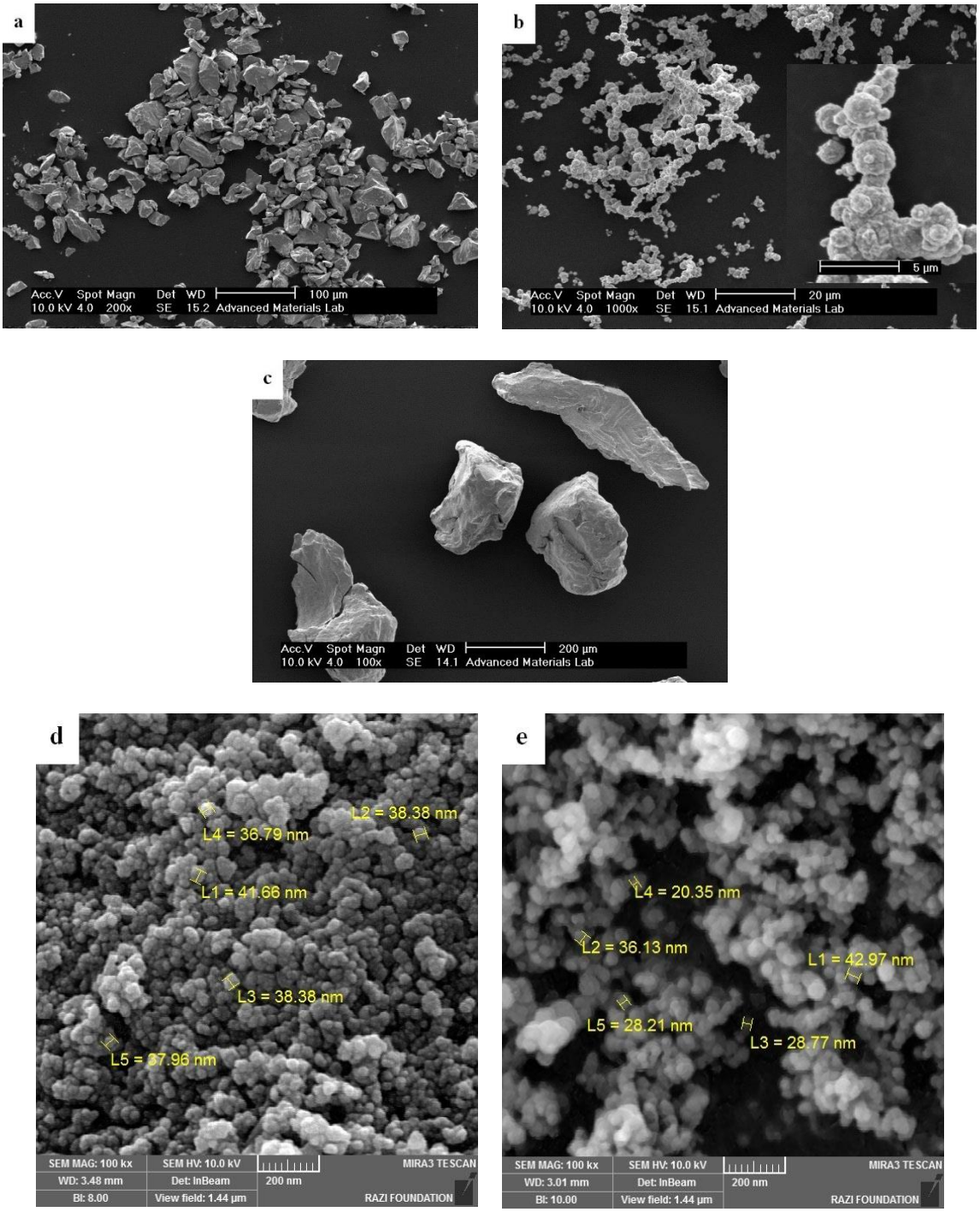

Figure. 1. The morphology of starting powders: (a) titanium, (b) nickel, (c) chromium, (d) Al_2O_{3np}, and (e) SiC_{np}.

In order to compare the effects of the nanoparticles on the resultant morphology of metals, the ball-milling process was applied with 20g of pure metals for 2, 6, and 24 hours. For this purpose,

25 wt. % Al_2O_3 and 25 wt. % SiC powders were separately added to the metals and blended for the pre-determined set times. The milling process for all the prepared powders was performed at a constant milling speed of 250 rpm under argon atmosphere (with purity of 99.99%) with a Sepahan 84D planetary ball mill. The ball to powder weight ratio of 5:1 and the hardened steel balls with different diameters (5, 10, and 20 mm) were used. Stearic acid at 1.5 wt. % was used as a process control agent (PCA) to decrease the agglomeration (Ramezani and Neitzert 2012). A two-hour milling followed by a 30 min stop cycle was applied to prevent excessive temperature increase in the milled powders.

The phase composition of the samples after ball milling was characterized using X-ray diffraction (XRD, Bruker's D8 advance system, Germany) with Cu Kα (λ=0.15405 nm) radiation source. Microstructural characterizations were performed using two kinds of scanning electron microscopes (SEM, Cam Scan MV2300 and SEM, Philips XL 30), and a field emission scanning electron microscopy (FESEM-Mira Tescan). The distribution and average powder particle sizes were estimated from the SEM and FESEM images by ImageJ software (version 1.47).

3. Results and discussion

The main purpose of this study was to determine and understand the microstructure evolution of ball-milled titanium, nickel, and chromium matrix composites reinforced with nano-alumina and nano-SiC particles. In order to illustrate the effect of the nanoparticle presence, the morphological changes of the pure metals during ball milling were also investigated. The effect of ball milling on the titanium powders, after 2 and 6 hours is shown in Figs. 2(a) and (b), respectively. It can be observed that particles were fragmented into finer particles after 2 hours but by persistent milling up to 6 hours the particles were flatten and their average particle size

appears to be increased. Figure 3 shows considerable changes in morphology of the Ti powders after 24 hours milling. After this period, many of the flattened powders welded to each other, fragmented particles were entrapped between these layers, and some separated fine particles were also revealed.

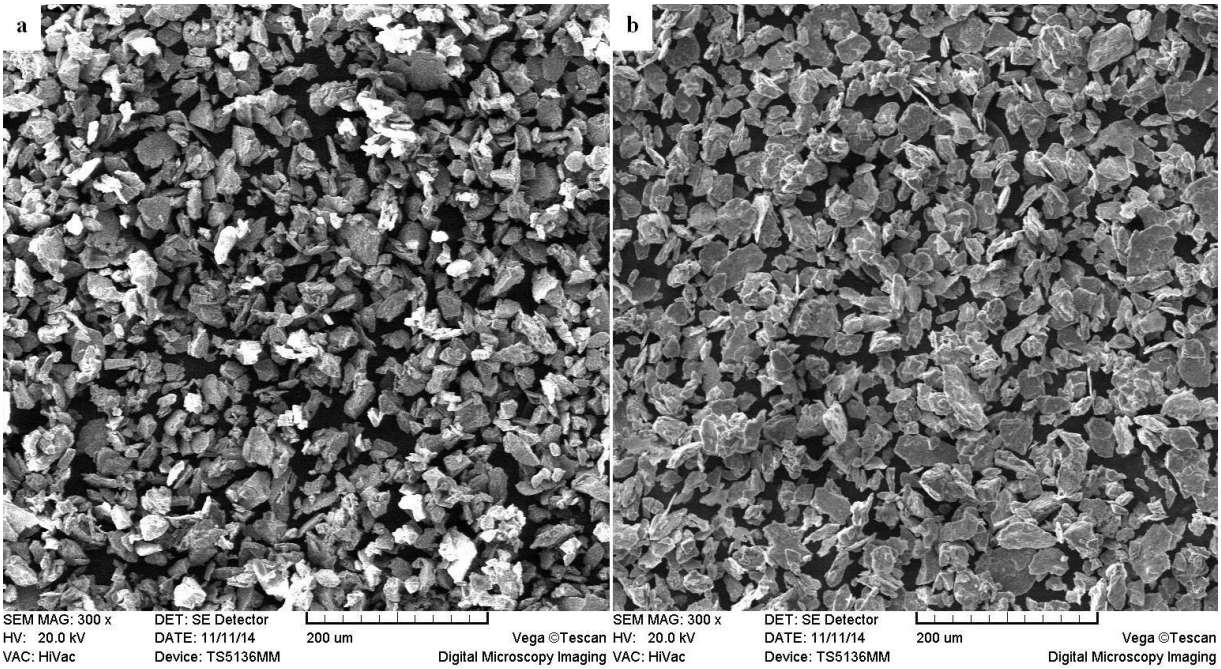

Figure. 2. SEM micrographs of Ti powders milled for (a) 2h and (b) 6h.

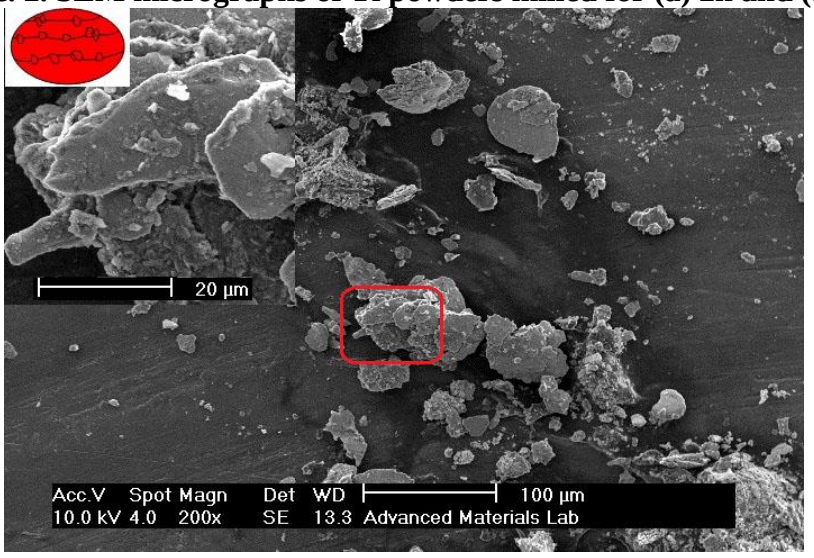

Figure. 3. SEM micrographs of Ti powders after 24 hours milling.

The ball milled nickel powders after 2 and 6 hours are shown in Figures 4(a) and (b). They exposed severe cold welding after 2 hours milling, leading to a considerable particle size increment. By increasing the milling time up to 6 hours, the particles were broken down into finer fragments, in contrast with Ti powders, in which the mean particles size tended to increase with milling time. Flattened powders, with entrained fine fragmented particles due to cold working with an increased average particle size were formed after 24 hours for the Ni powders, see Figure 5. The Ni powder matrix showed considerabley more reduction in average particle size after 6 hours in comparison with the Ti powder matrix. This can be attributed to the higher potential of the FCC based Ni structure to work harden, and therefore fracture more, compared to the hexagonal based Ti crystal structure (Nes 1997). The work-hardeing exponent of FCC metals is considerably higher than those of BCC and HCP metals, meaing that they have required potential for receiving a high value of dislocation density for hardening. Work-hardeing makes a metal to become less ductile and more brittle. Therefore, a higher value of particle fracturing will occur during plastic deformation (Nes 1997).

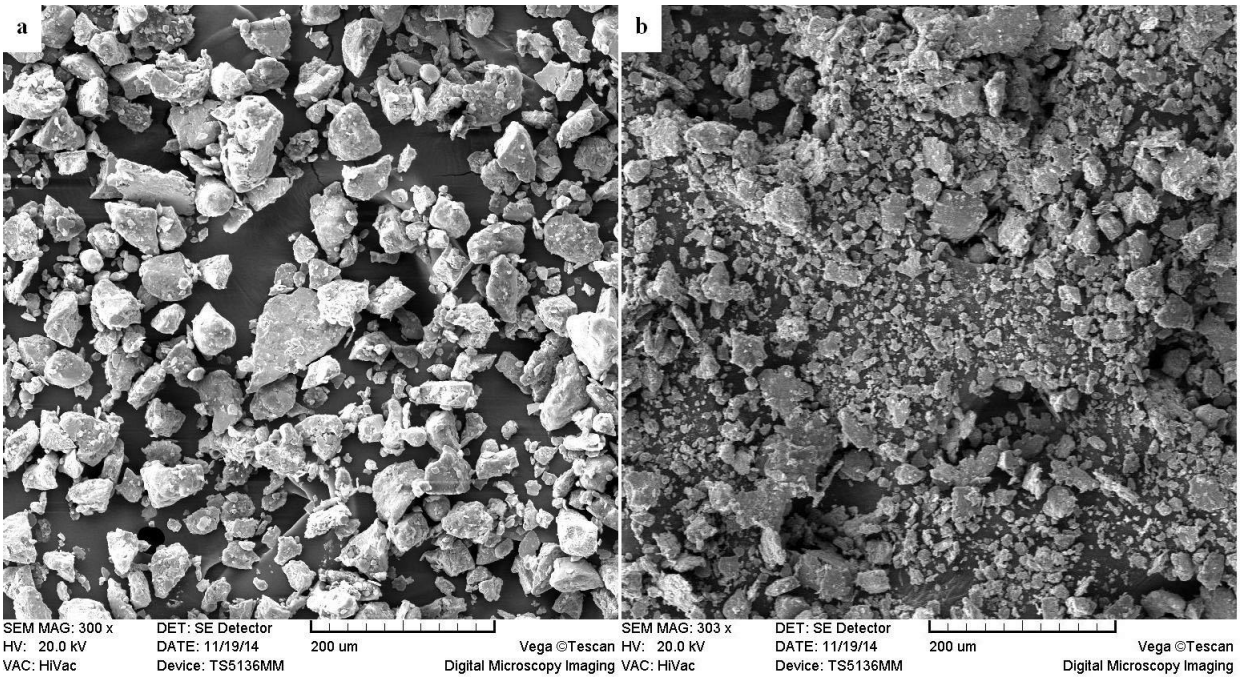

Figure. 4. SEM micrographs of Ni powders milled for (a) 2h and (b) 6h.

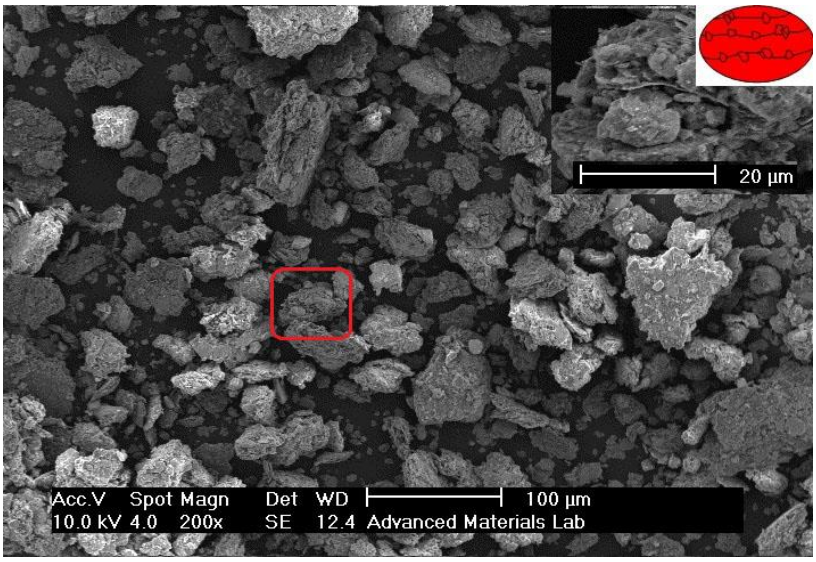

Figure. 5. SEM micrographs of Ni powders after 24 hours milling.

The coarse irregular particles of as-received chromium (with BCC atomic structure) formed finer particles after 2 and 6 hours of milling (Figure 6), and simultaneously a flake-like morphology was obtained. Figure 7 presents the microstructure of the 24-hour milled Cr powders. The embedded fine fragments between the cold welded layers can be seen as well as the tendency of

the layers to agglomerate, leading to a decrease in the surface energy of the powders. Comparing figures 6 and 7, it can be seen that the average particle size had no significant variation between 2 hours and 24 hours of milling period.

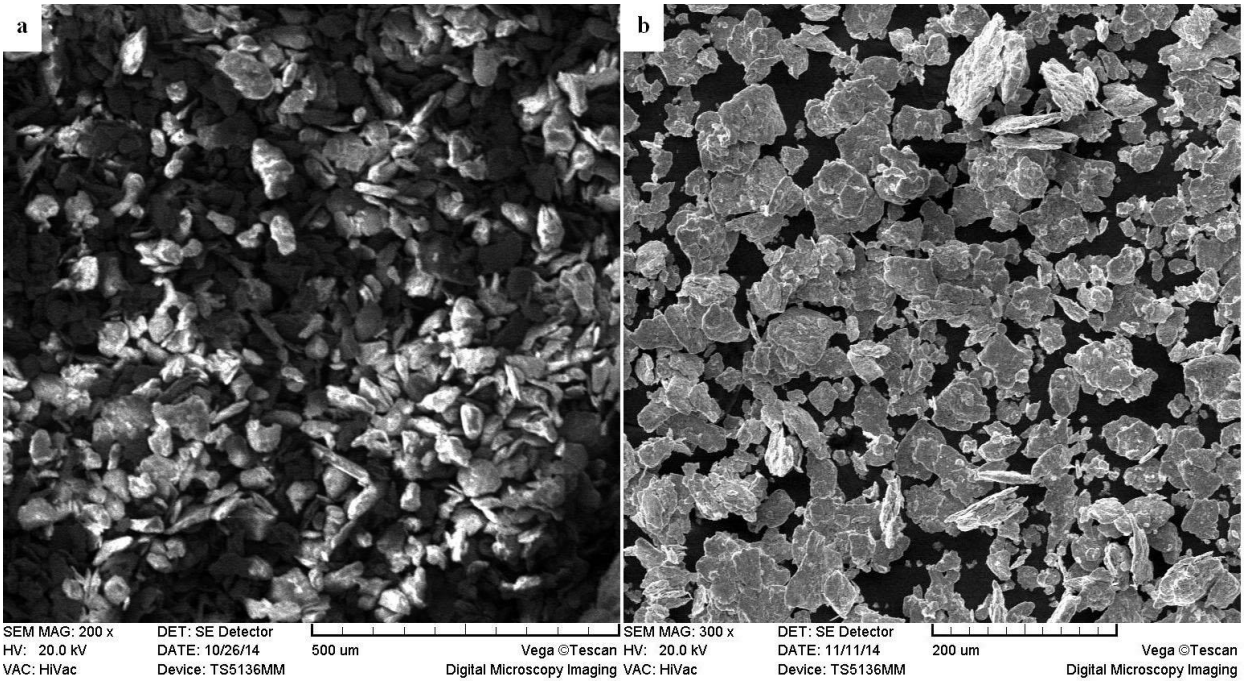

Figure. 6. SEM micrographs of Cr powders milled for (a) 2h and (b) 6h.

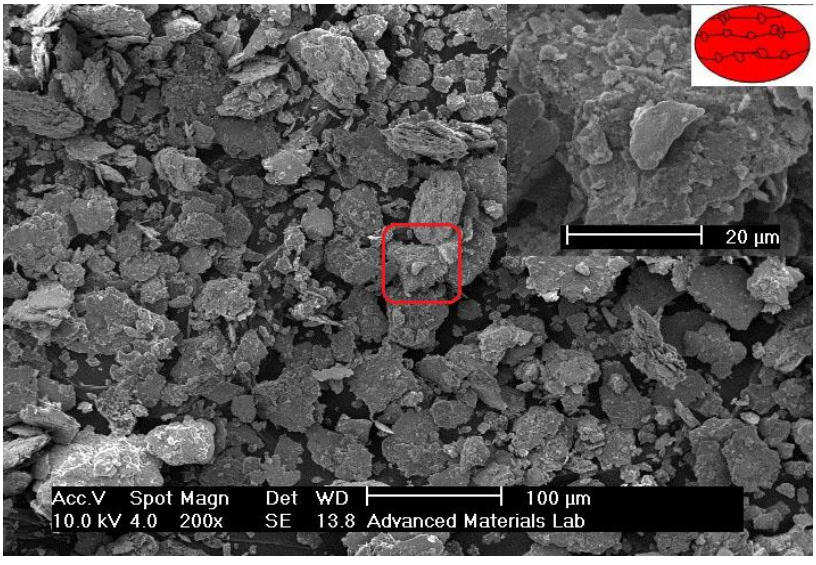

Figure. 7. SEM micrographs of Cr powders after 24 hours milling.

The chemical composition of composite powders milled for 6 and 12 hours were recorded via XRD. Figure 8(a) shows the Ti-Al_2O_3 powder XRD resulrs after milling for 6 and 12 hours. The strong peaks of titanium as well as less pronounced peaks of Al_2O_{3np} were detected after 6 hours. Reaction between the alumina and Ti can also be seen to have occurred as the corresponding peaks of TiO can be seen for 12 hours ball-milled powders. This indicates that Ti is not thermodynamically stable with alumina during intensive milling. It can be observed that the relevant peaks, which were shown in Fig. 8a after 12h, have a very low intensity and a higher width, and considerable background, showing the low crystallite sizes of the produced products after reaction (Mousavian, Sharafi, and Shariat 2011). Figure 8(b) shows the XRD analysis of Ni-Al_2O_3 milled for 6 and 12 hours, in which just the peaks of nickel and alumina were recorded. The XRD analysis of the Cr-Al_2O_3 powder is shown in Figure 8(c), in which there is no evidence for alumina peaks. It is not clear that why alumina peaks were hidden for this sample.

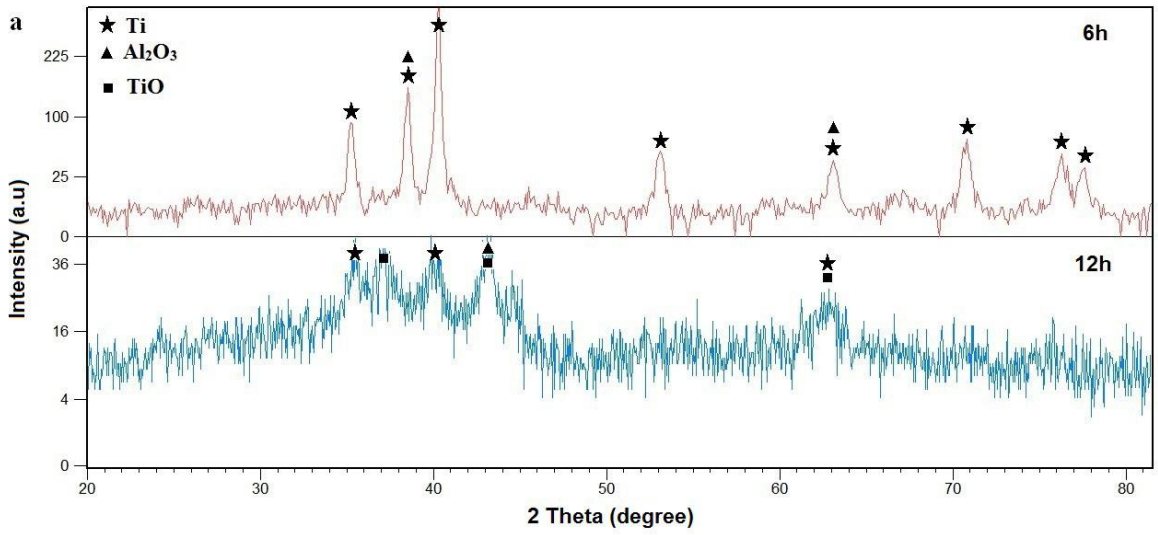

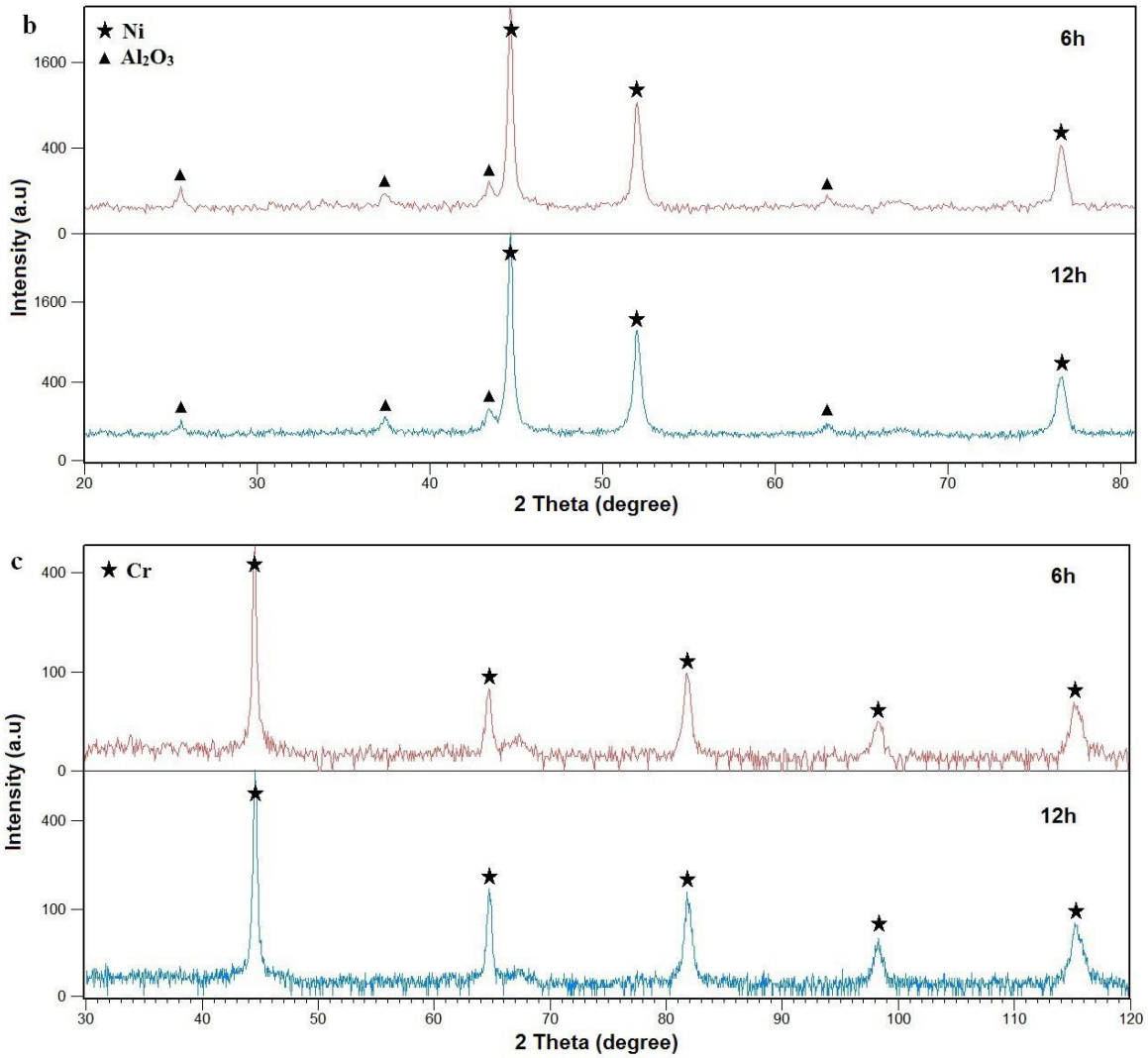

Figure. 8. XRD patterns of the milled powders after 6 and 12 hours for (a) Ti-Al2O3, (b) Ni-Al2O3, and (c) Cr-Al2O3 mixtures.

Based on the XRD results, FESEM further imaging was performed of the powders milled for 2 and 6 hours. Figures 9 to 11 show the FESEM images of the Ti, Ni and Cr metal matrices, respectively, reinforced with Al_2O_{3np}. The FESEM images are presented for the composites milled for 2 hours (Figures 9(a), 10(a) and 11(a) (low magnification), 9(b), 10(b) and 11(b) (high magnification)), and 6 hours (Figures 9(c), 10(c), and 11(c) (low magnification), 9(d), 10(d), and 11(d) (high magnification)). Some important points can be drawn from the powder FESEM images before and after milling. First, by comparing of Figure 2 with Figures 9(a) and (c); Figure

4 with Figures 10(a) and (c); and Figure 6 with Figures 11(a) and (c); it is revealed that the presence of the nanoparticles significantly changed the morphology and particle size of metal powder particles. A much-reduced metal particle size was obtained for the composite powders compared with the pure metals after milling. It should be noted that the particles size of Ti composite had no considerable difference with the pure Ti powders until 2 hours of milling. It has been indicated in previous work, that nano ceramic particles highly affect the work hardening rate of metallic powders, in particular for FCC and BCC metals that have a higher potential for work-hardening (Meyers, Mishra, and Benson 2006).

Secondly, as shown in Figures 9(b), 10(b), and 11(b), disagglomeration of the nanoparticles occurred from the initial stages of the milling process, which is in contrast with some previously published results (Salahi and Rajabi 2016). It can be observed that a uniform distribution of nanoparticles on the outer surface of powders was mostly achieved after just 2 hours of milling (Figures 9(a,b), 10(a,b), and 11(a,b)). The presence of agglomerated nanoparticles for both 2 and 6 hours milled powders highlights the fact that increasing the milling time had no positive effect on improving the nanoparticle distribution, when 25 wt. % nano-reinforcement is used.

Thirdly, the nickel-based nanocomposite powders were much finer than Ti and Cr based composite powders, while the pure metal powders of Ti seems to contain smaller particle size after milling, indicating the effect of nanoparticles on the acceleration of work hardening for nickel powders. It is reported in the literature that the work hardening exponent of FCC metals is higher than for BCC, both of which are higher than HCP metals (Meyers and Chawla 2009). Nickel is therefore the most microstructurally effected metal by presence of the nanoparticles.

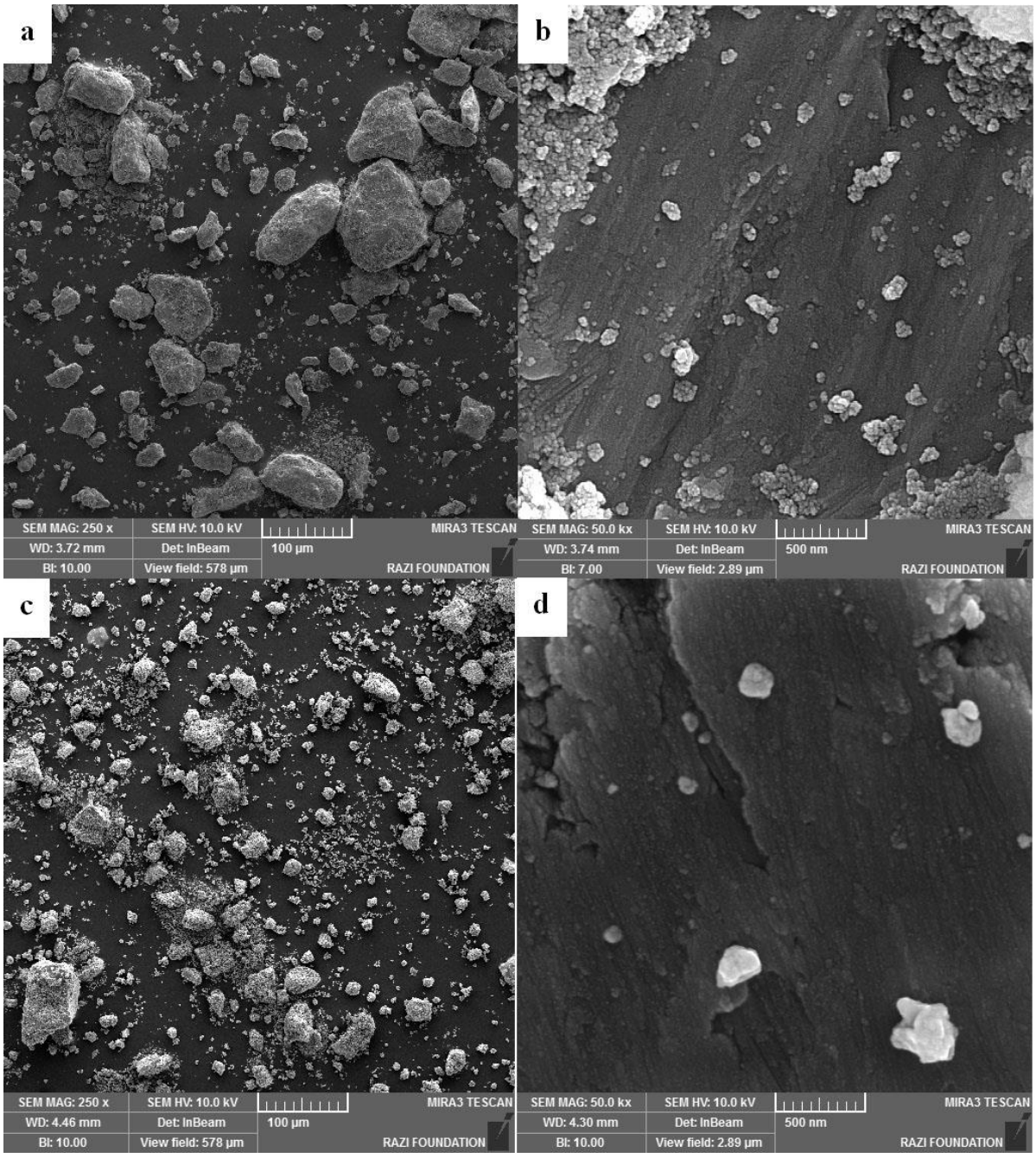

Figure. 9. FESEM images of Ti-Al2O3 powders milled for (a, b) 2h and (c, d) 6h, (a, c) low magnification, and (b, d) high magnification.

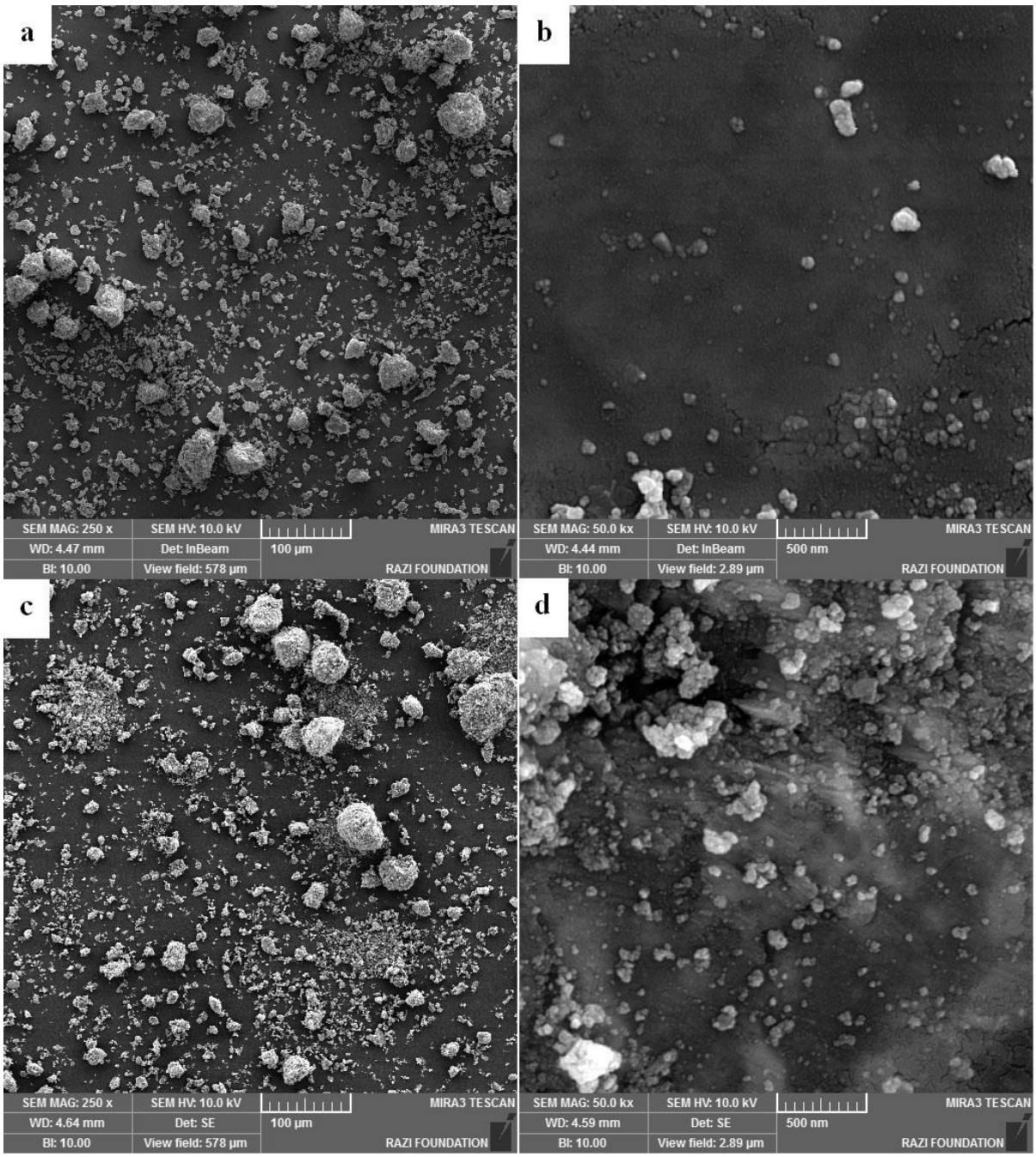

Figure. 10. FESEM images of Ni-Al2O3 powders milled for (a, b) 2h and (c, d) 6h, (a, c) low magnification, and (b, d) high magnification.

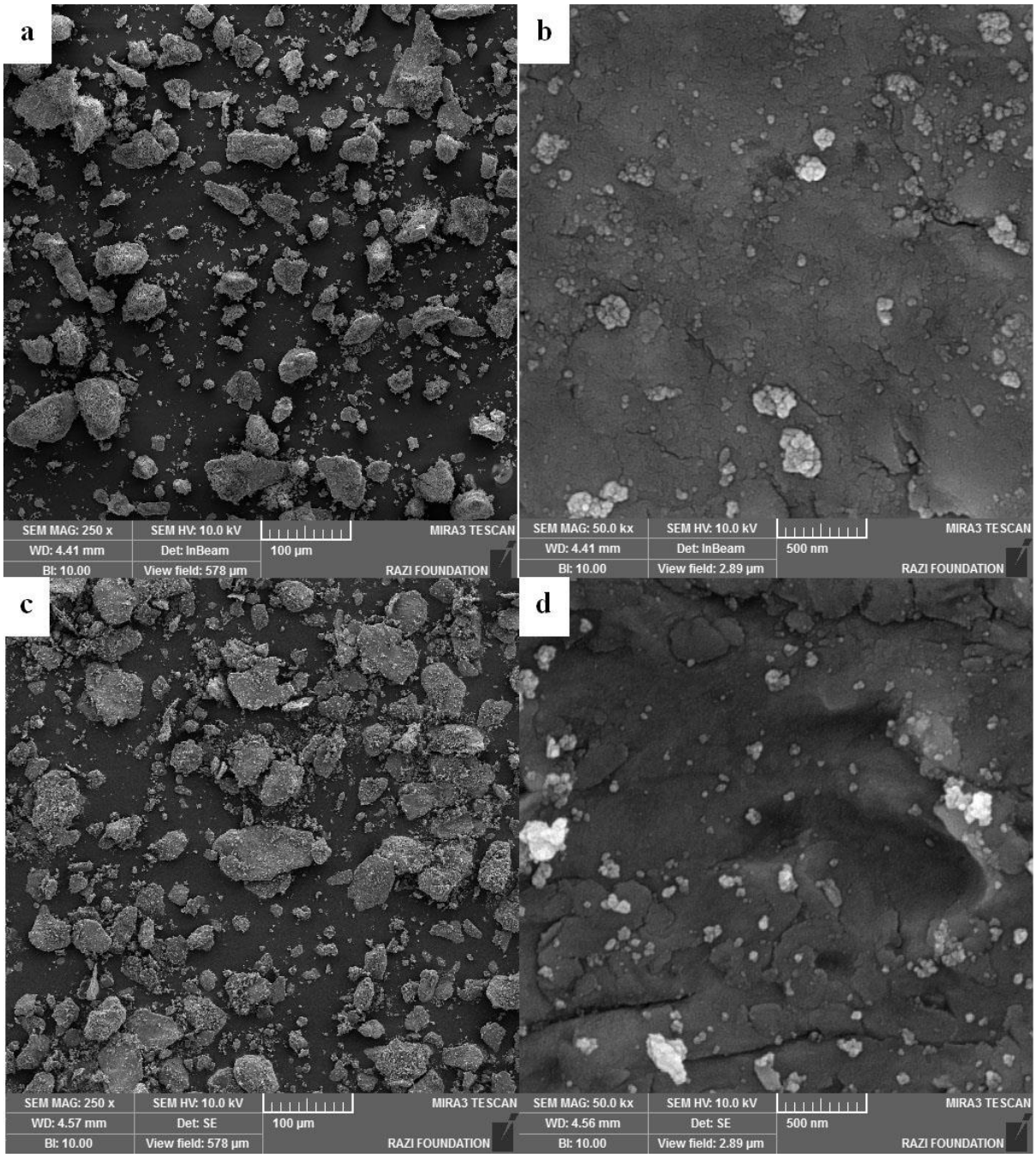

Figure. 11. FESEM images of Cr-Al2O3 powders milled for (a, b) 2h and (c, d) 6h, (a, c) low magnification, and (b, d) high magnification.

In this study, SiC nanoparticles were also used as reinforcement to show the effect of nanoparticle type on the microstructure and morphology of composite powders. XRD analysis of 24-hour milled Ti, Ni, and Cr based nanocomposites reinforced with SiC is shown in Figures 12(a-c), respectively. It can be seen there is no evidence of reaction between matrices and SiC.

This shows that ball milling of SiC_{np} with these metals might not lead to a detrimental reaction during composite manufacturing at least until up to a 24h period of milling.

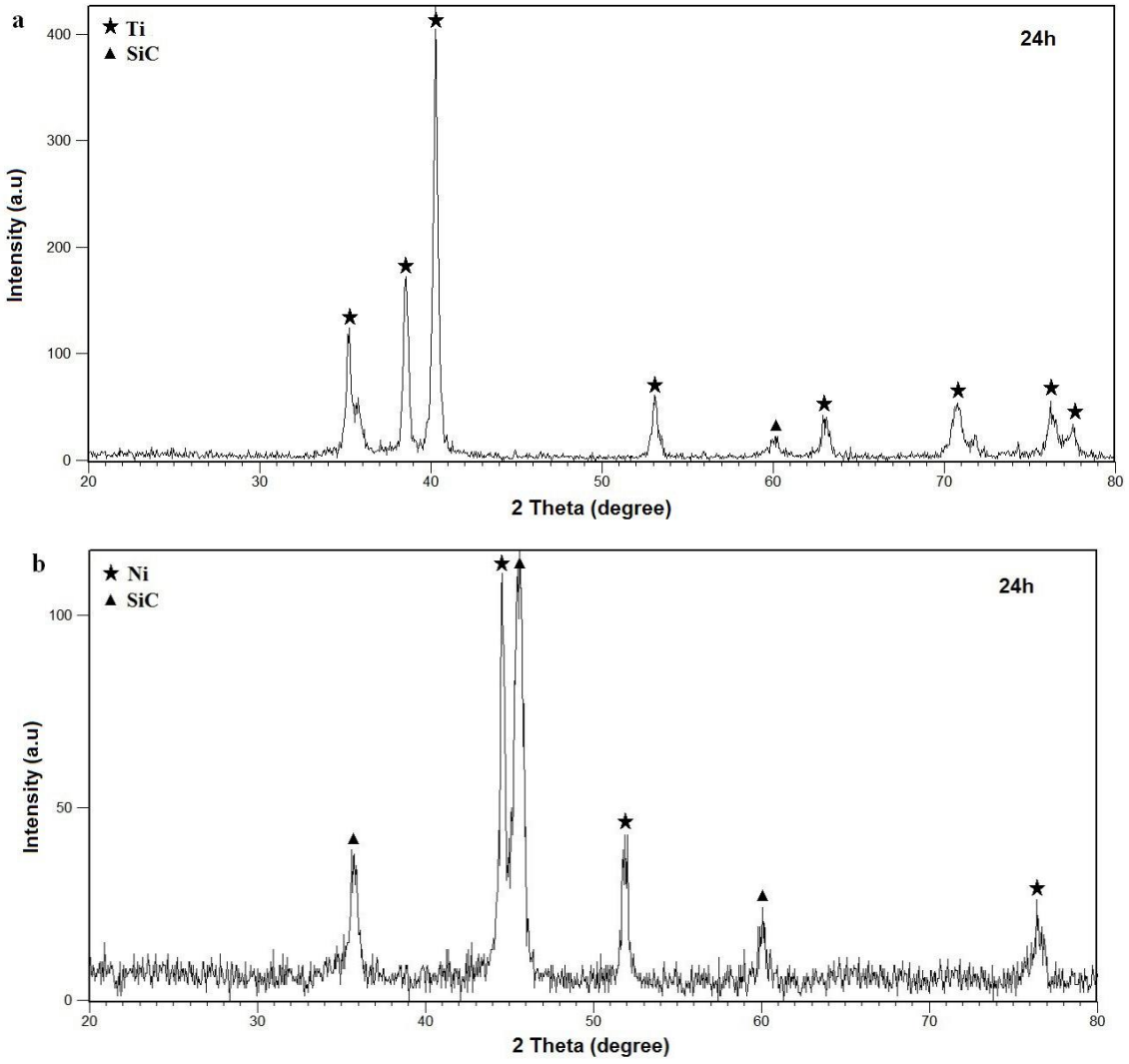

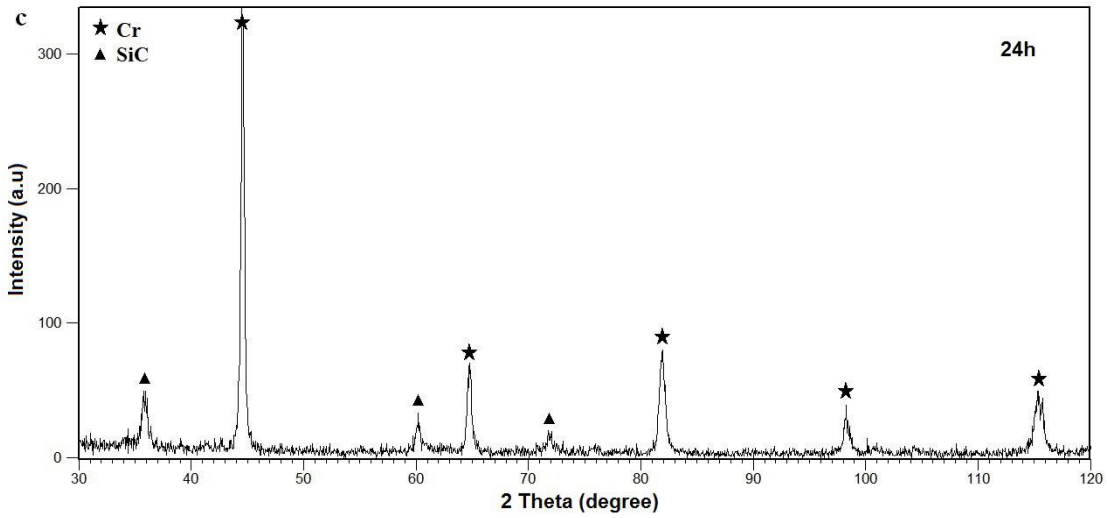

Figure. 12. XRD analysis of the milled powders after 24 hours for (a) Ti-SiC, (b) Ni-SiC and (a) Cr-SiC.

Based on the XRD analysis, FESEM further imaging was completed for the 24-hour milled powders. No significant microstructural difference is observed in Figure 13 when compared with those shown in Figures 9, 10, and 11. Therefore, by changing the mechanical properties of ceramic nanoparticles, no change might be observed in the case of distribution of nanoparticles and/or morphology and average particle size of composite powders, when 25 wt. % nanoparticles are used. Irrespective of refinement of composite powders in the presence of reinforcing SiC phase, some agglomerated ceramic particles with a metallic link (as shown in the schematic of Figures 13(a), (b), and (c)) were again observed. Very little differenece was observed between the distribution of nanoparticles between the samples.

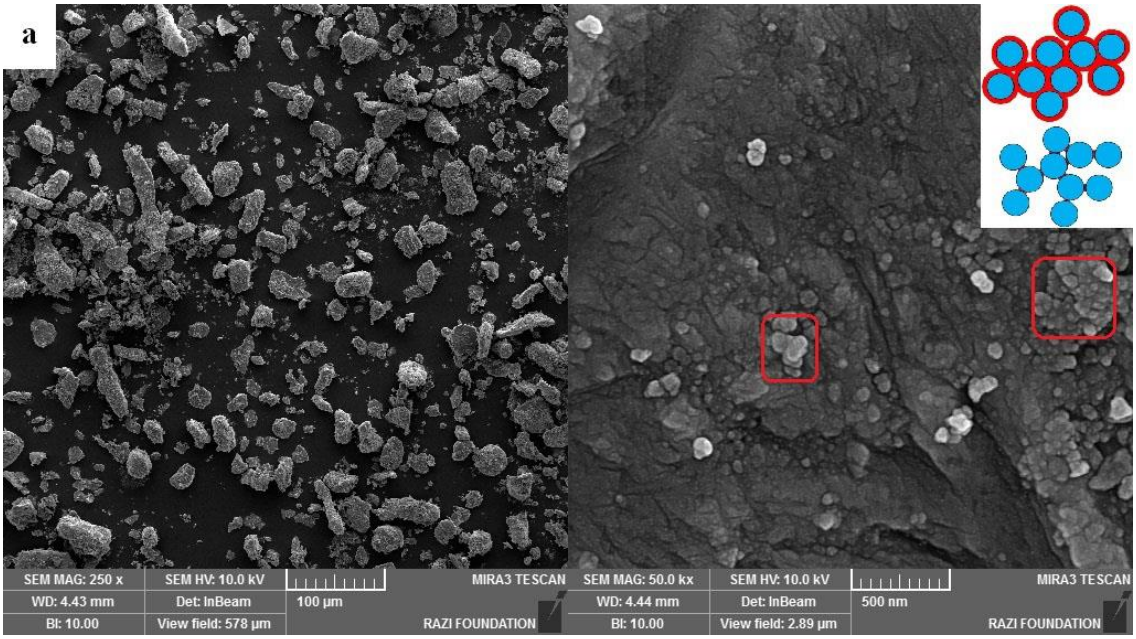
a
SEM MAG: 250 x
SEM HV: 10.0 kV
MIRA3 TESCAN
WD: 4.43 mm
Det: InBeam
100 µm
BI: 10.00
View field: 578 µm
RAZI FOUNDATION
SEM MAG: 50.0 kx
SEM HV: 10.0 kV
MIRA3 TESCAN
WD: 4.44 mm
Det: InBeam
500 nm
BI: 10.00
View field: 2.89 µm
RAZI FOUNDATION

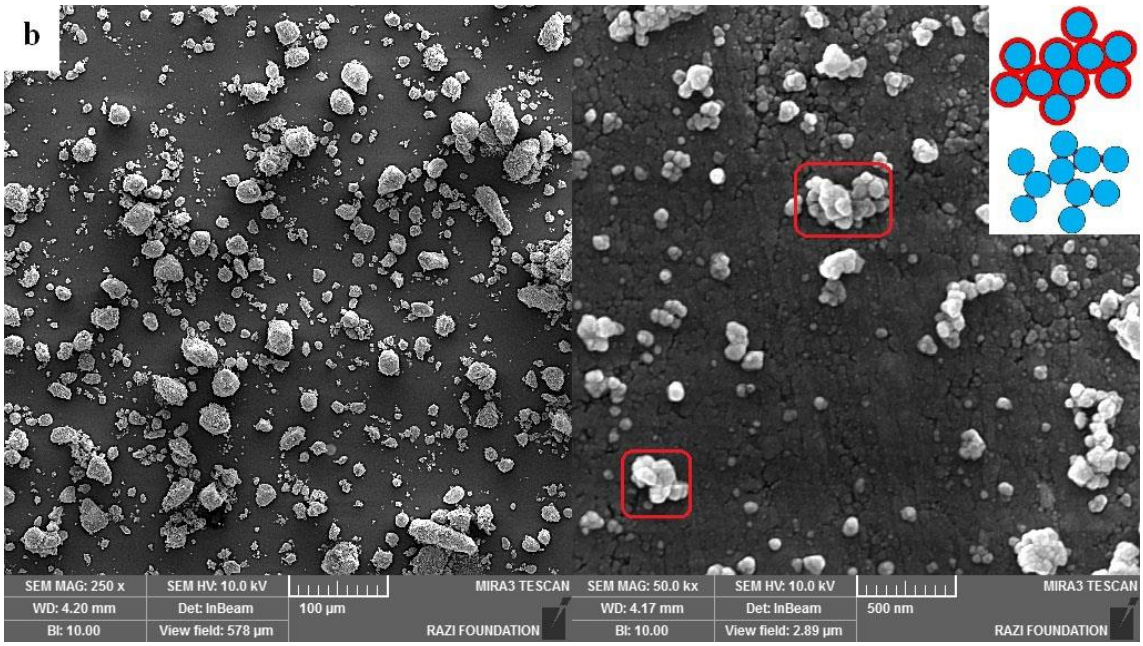
b
SEM MAG: 250 x
SEM HV: 10.0 kV
MIRA3 TESCAN
WD: 4.20 mm
Det: InBeam
100 µm
BI: 10.00
View field: 578 µm
RAZI FOUNDATION
SEM MAG: 50.0 kx
SEM HV: 10.0 kV
MIRA3 TESCAN
WD: 4.17 mm
Det: InBeam
500 nm
BI: 10.00
View field: 2.89 µm
RAZI FOUNDATION

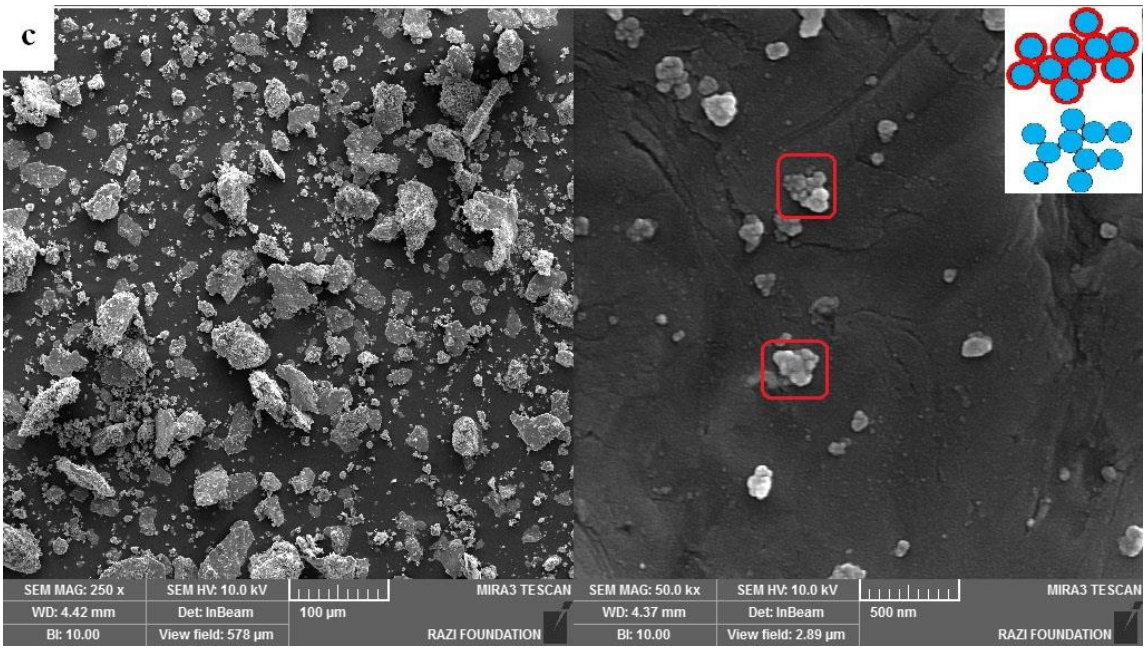

Figure. 13. FESEM images of the milled powders after 24 hours for (a) Ti-SiC, (b) Ni-SiC and (a) Cr-SiC.

Figure 14 presents a summary of the various microstructures and morphologies obtained in this study. It can be observed that by increasing the milling time, various composite powders with different particle sizes were obtained, containing single and agglomerated ceramic nanoparticles inside and outside of the metal powder particles as well as some fragmented metallic powders.

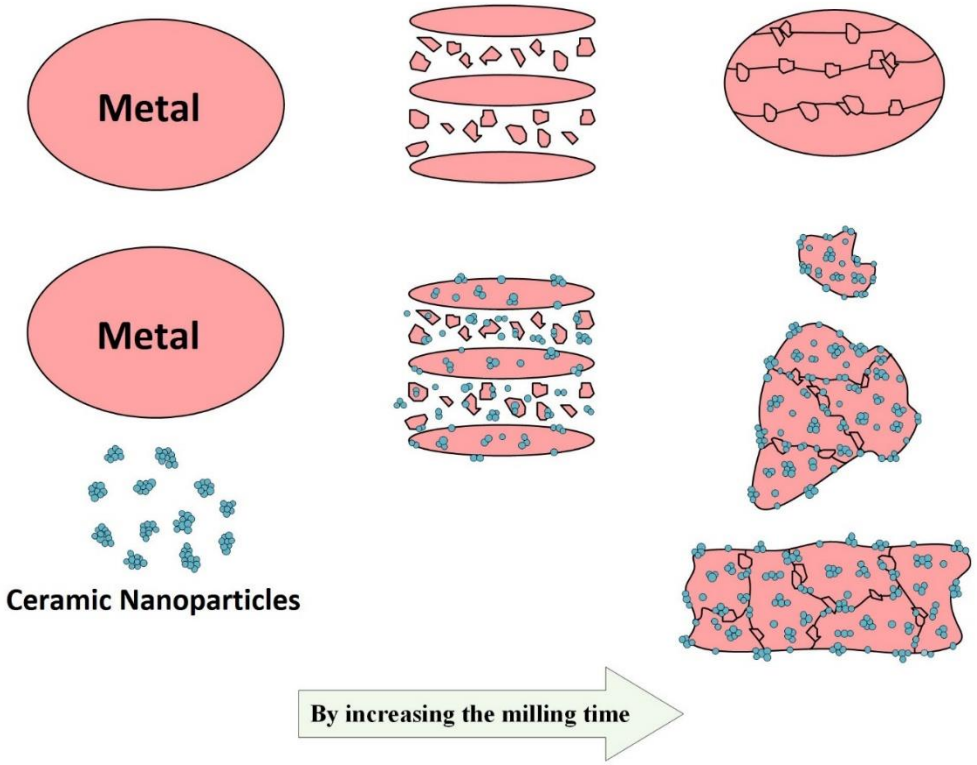

Figure. 14. The schematic of the obtained MMNCs morphologies after ball-milling process by increasing the milling time.

Finally, in order to clarify the effect of metallic type, ceramic type, and milling time on the value of average particles size and their distribution, image analysis was used. Figures 15, 16, and 17 show the image analysis results. It can be seen that no work hardening and fragmentation occurred for titanium and almost none for the chromium particles by increasing the milling time, while the nickel powders were exposed to severe refinement between 2 and 6 hours ball milling. Although, ceramic nanoparticles caused a severe reduction in the average particle size of all the matrices, however, nickel matrix experienced the highest particle size reduction, in particular after 6 hours milling with alumina nanoparticles present.

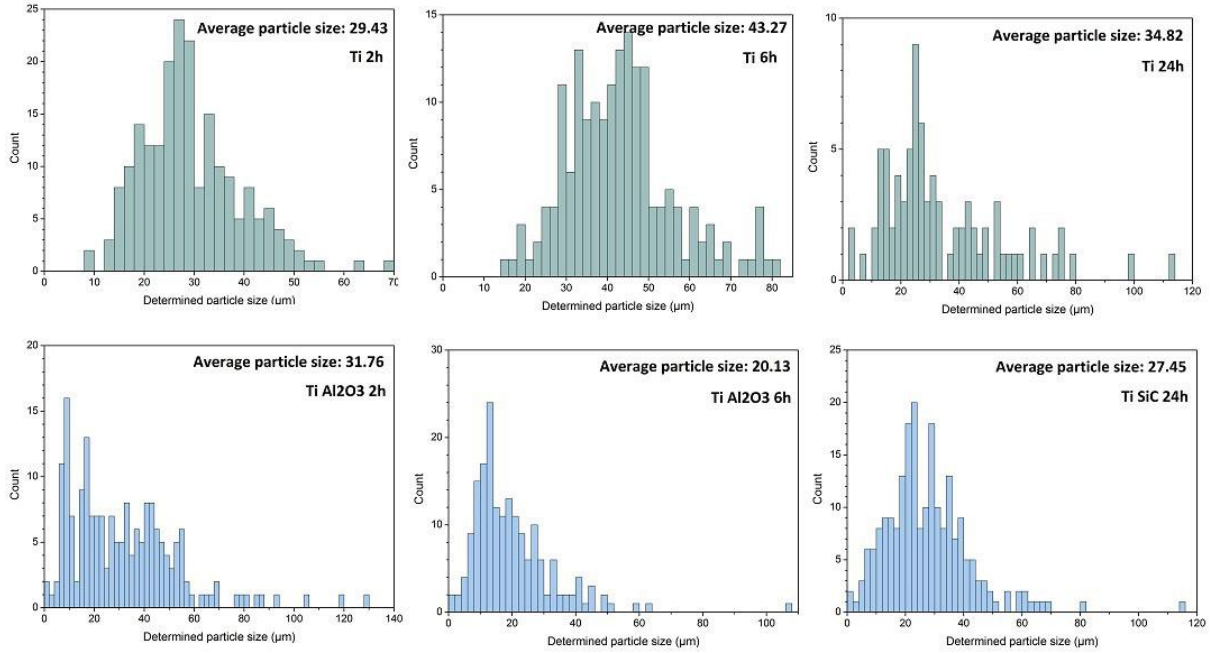

Figure. 15. Image analysis of titanium powders as well as their composites.

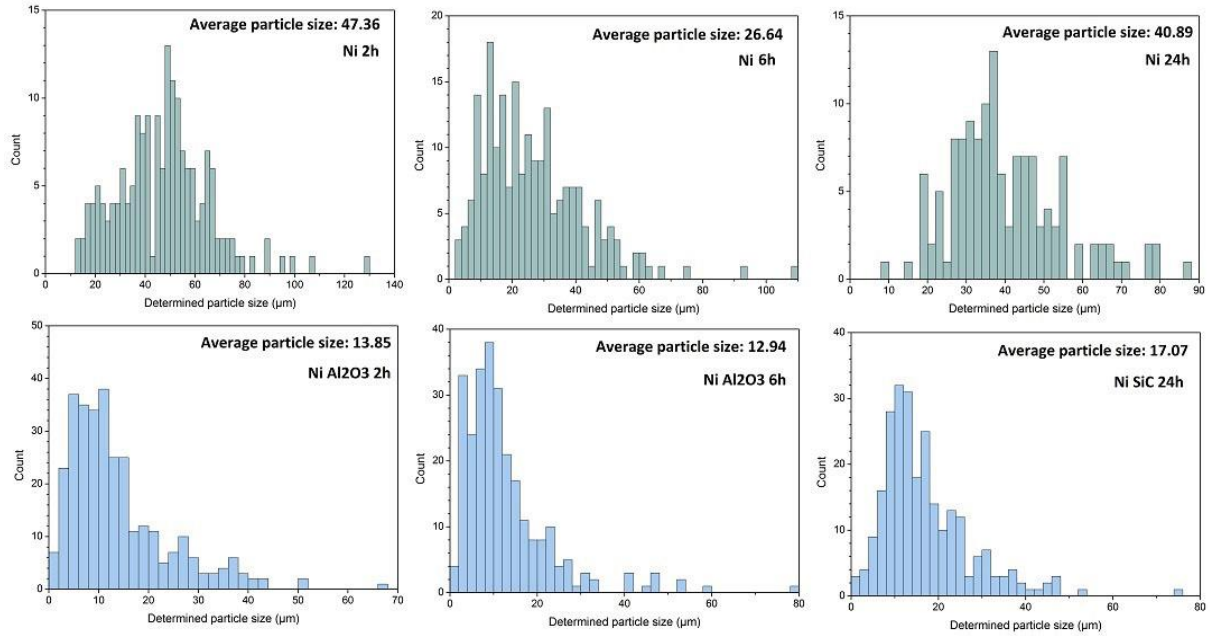

Figure. 16. Image analysis of nickel powders as well as their composites.

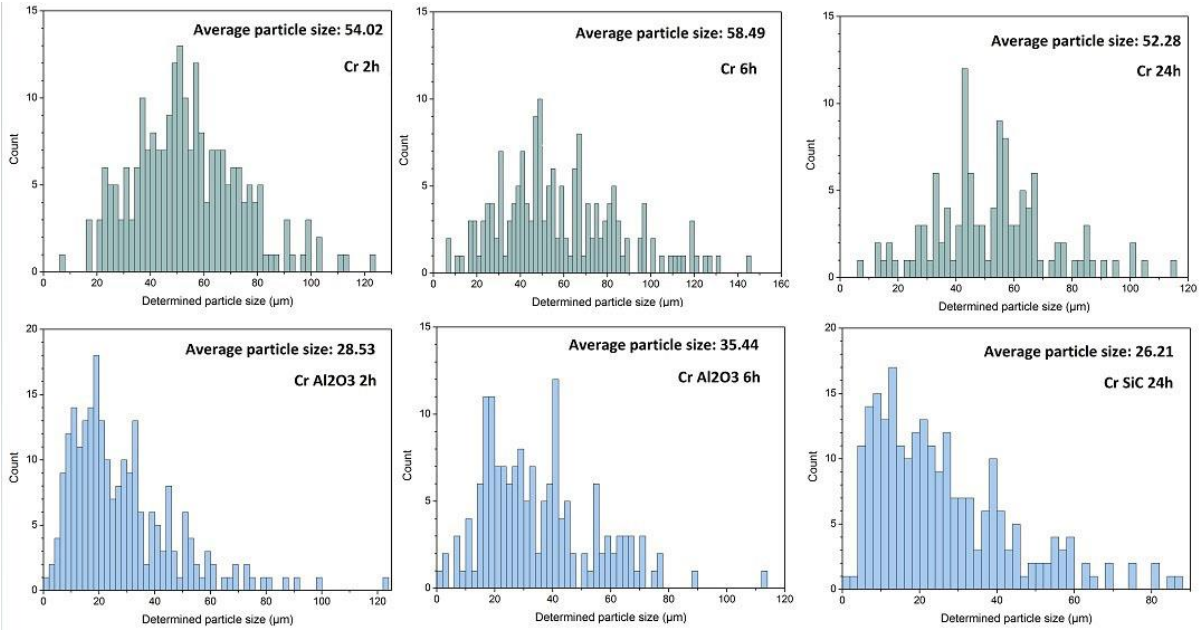

Figure. 17. Image analysis of chromium powders as well as their composites.

4. Conclusion

The effect of metallic matrix, ceramic nanoparticle, and milling time were evaluated on the microstructure and morphology of metal matrix nanocomposites. From the experimental results, the followings could be drawn:

1. Depending on the atomic structure of metal matrices, various morphologies and microstructures were obtained. The type of metals is also important for the effect of nanoparticles on the microstructure of composite powders.

2. Nickel powders with the FCC structure experienced the highest particle size reduction compared with the other metals.

3. The type of ceramic nanoparticles did not considerably effective the morphology of composite powders and distribution of nanoparticles.

4. By increasing the milling time, no improved distribution of nanoparticles was obtained.

References

Allison, John E, and Gerald S Cole. 1993. Metal-matrix composites in the automotive industry: opportunities and challenges. *JoM* 45 (1):19-24.

Bernoosi, Samaneh, Rasoul Azari Khosroshahi, and Reza Taherzadeh Mousavian. 2014. Mechanical properties of hot-pressed Al-4.5 wt.% Cu/WC composite. *Journal of Ultrafine Grained and Nanostructured Materials* 47 (2):63-70.

Boostani, A Fadavi, R Taherzadeh Mousavian, S Tahamtan, S Yazdani, R Azari Khosroshahi, D Wei, J Xu, X Zhang, and ZY Jiang. 2016. Solvothermal-assisted graphene encapsulation of SiC nanoparticles: A new horizon toward toughening aluminium matrix nanocomposites. *Materials Science and Engineering: A* 653:99-107.

Boostani, A Fadavi, R Taherzadeh Mousavian, S Tahamtan, Siamak Yazdani, R Azari Khosroshahi, Dongbin Wei, Jian Zhong Xu, Dianyao Gong, XM Zhang, and ZY Jiang. 2015. Graphene sheets encapsulating SiC nanoparticles: A roadmap towards enhancing tensile ductility of metal matrix composites. *Materials Science and Engineering: A* 648:92-103.

Boostani, A Fadavi, S Tahamtan, ZY Jiang, Dongbin Wei, Siamak Yazdani, R Azari Khosroshahi, R Taherzadeh Mousavian, Jianzhong Xu, X Zhang, and Dianyao Gong. 2015. Enhanced tensile properties of aluminium matrix composites reinforced with graphene encapsulated SiC nanoparticles. *Composites Part A: Applied Science and Manufacturing* 68:155-163.

Boostani, A Fadavi, S Yazdani, R Taherzadeh Mousavian, S Tahamtan, R Azari Khosroshahi, D Wei, D Brabazon, JZ Xu, XM Zhang, and ZY Jiang. 2015. Strengthening mechanisms of graphene sheets in aluminium matrix nanocomposites. *Materials & Design* 88:983-989.

Casati, Riccardo, and Maurizio Vedani. 2014. Metal matrix composites reinforced by nano-particles—a review. *Metals* 4 (1):65-83.

de Oliveira, Leiliane Alves, Uílame Umbelino Gomes, Ariadne Souza Silva, and Emanuel João Batista. 2015. Metal Matrix Composites Added of Nanostructured Tantalum Carbide.

Forouzan, MR, R Taherzadeh Mousavian, T Sharif, and YA Afkham. 2015. A three-step synthesis process of submicron boron carbide powders using microwave energy. *Journal of Thermal Analysis and Calorimetry* 122 (2):579-588.

Gajović, Andreja, Mirko Stubičar, Mile Ivanda, and Krešimir Furić. 2001. Raman spectroscopy of ball-milled TiO 2. *Journal of Molecular Structure* 563:315-320.

He, Fei, Qingyou Han, and Mark J Jackson. 2008. Nanoparticulate reinforced metal matrix nanocomposites-a review. *International Journal of Nanoparticles* 1 (4):301-309.

Ibrahim, IA, FA Mohamed, and EJ Lavernia. 1991. Particulate reinforced metal matrix composites—a review. *Journal of materials science* 26 (5):1137-1156.

Kaczmar, JW, K Pietrzak, and W Włosiński. 2000. The production and application of metal matrix composite materials. *Journal of Materials Processing Technology* 106 (1):58-67.

Khakbiz, M, and F Akhlaghi. 2009. Synthesis and structural characterization of Al–B 4 C nano-composite powders by mechanical alloying. *Journal of Alloys and Compounds* 479 (1):334-341.

Mahboob, H, SA Sajjadi, and SM Zebarjad. 2011. Influence of nanosized Al2O3 weight percentage on microstructure and mechanical properties of Al-matrix nanocomposite. *Powder metallurgy* 54 (2):148-152.

Meyers, Marc A, and Krishan Kumar Chawla. 2009. *Mechanical behavior of materials*. Vol. 2: Cambridge university press Cambridge.

Meyers, Marc A, A Mishra, and David J Benson. 2006. Mechanical properties of nanocrystalline materials. *Progress in materials science* 51 (4):427-556.

Miracle, DB. 2005. Metal matrix composites–from science to technological significance. *Composites science and technology* 65 (15):2526-2540.

Mobasherpour, I, AA Tofigh, and M Ebrahimi. 2013. Effect of nano-size Al 2 O 3 reinforcement on the mechanical behavior of synthesis 7075 aluminum alloy composites by mechanical alloying. *Materials Chemistry and Physics* 138 (2):535-541.

Mohanty, Pragyan, Kampal Mishra, Ranadhir Bosu, and Payodhar Padhi. 2014. Achieving uniform nanoparticle distributions of bulk Al/Al 2 O 3 metal matrix nanocomposites. *International Journal of Nanomanufacturing* 10 (5-6):478-488.

Mojtaba, Ghasemi, Marandi Seyed Morteza, Tahmooresi Majid, Kamali Reza Jalal, and Taherzade Reza. 2012. Modification of stone matrix asphalt with nano-SiO2. *J. Basic Appl. Sci. Res* 2 (2):1338-1344.

Mosleh, A, M Ehteshamzadeh, and R Taherzadeh Mousavian. 2014. Fabrication of an r-Al2Ti intermetallic matrix composite reinforced with α-Al2O3 ceramic by discontinuous mechanical milling for thermite reaction. *International Journal of Minerals, Metallurgy, and Materials* 21 (10):1037-1043.

Mousavian, R Taherzadeh, N Azizi, Zhengyi Jiang, and A Fadavi Boostani. 2014. Effect of Fe2O3 as an accelerator on the reaction mechanism of Al–TiO2 nanothermite system. *Journal of Thermal Analysis and Calorimetry* 117 (2):711-719.

Mousavian, R Taherzadeh, R Azari Khosroshahi, S Yazdani, D Brabazon, and AF Boostani. 2016. Fabrication of aluminum matrix composites reinforced with nano-to micrometer-sized SiC particles. *Materials & Design* 89:58-70.

Mousavian, R Taherzadeh, S Sharafi, MR Roshan, and MH Shariat. 2011. Effect of mechanical activation of reagents' mixture on the high-temperature synthesis of Al2O3–TiB2 composite powder. *Journal of thermal analysis and calorimetry* 104 (3):1063-1070.

Mousavian, R Taherzadeh, S Sharafi, and MH Shariat. 2011. Microwave-assisted combustion synthesis in a mechanically activated Al–TiO 2–H 3 BO 3 system. *International Journal of Refractory Metals and Hard Materials* 29 (2):281-288.

Mousavian, R Taherzadeh, S Sharafi, and MH Shariat. 2011. Preparation of nano-structural Al2O3-TiB2 in-situ composite using mechanically activated combustion synthesis followed byintensive milling. *Iranian Journal of Materials Science and Engineering* 8 (2):1-9.

Mousavian, Reza Taherzadeh, Rasoul Azari Khosroshahi, Sasan Yazdani, and Dermot Brabazon. 2016 Manufacturing of cast A356 matrix composite reinforced with nano-to micrometer-sized SiC particles. *Rare Metals*: 1-9.

Nekouee, Kh A, RA Khosroshahi, R Taherzadeh Mousavian, and N Ehsani. 2015 Sintering behavior and microwave dielectric properties of SiO2–MgO–Al2O3–TiO2 ceramics. *Journal of Materials Science: Materials in Electronics*:1-6.

Nes, Erik. 1997. Modelling of work hardening and stress saturation in FCC metals. *Progress in Materials Science* 41 (3):129-193.

Ozdemir, Ismail, Sascha Ahrens, Silke Mücklich, and Bernhard Wielage. 2008. Nanocrystalline Al–Al 2 O 3p and SiC p composites produced by high-energy ball milling. *journal of materials processing technology* 205 (1):111-118.

Pramanik, Alokesh, and Guy Littlefair. 2013. Fabrication of nano-particle reinforced metal matrix composites. Paper read at Advanced Materials Research.

Ramezani, M, and T Neitzert. 2012. Mechanical milling of aluminum powder using planetary ball milling process. *JAMME* 55 (2):790-798.

Rivera, JL Hernández, JJ Cruz Rivera, V Paz del Ángel, V Garibay Febles, O Coreño Alonso, and R Martínez-Sánchez. 2012. Structural and morphological study of a 2024 Al–Al 2 O 3 composite produced by mechanical alloying in high energy mill. *Materials & Design* 37:96-101.

Rosas, G, R Esparza, HB Liu, JA Ascencio, and R Pérez. 2005. Preparation of AlFe nanoparticles by mechanical alloyed technique. *Journal of nanoscience and nanotechnology* 5 (12):2133-2137.

Salahi, E, and A Rajabi. 2016. Fabrication and characterisation of copper–alumina nanocomposites prepared by high-energy fast milling. *Materials Science and Technology*.

Suryanarayana, C, and Nasser Al-Aqeeli. 2013. Mechanically alloyed nanocomposites. *Progress in Materials Science* 58 (4):383-502.

Suryanarayana, C, E Ivanov, and VV Boldyrev. 2001. The science and technology of mechanical alloying. *Materials Science and Engineering: A* 304:151-158.

Suryanarayana, Challapalli. 2001. Mechanical alloying and milling. *Progress in materials science* 46 (1):1-184.

Valibeygloo, N, R Azari Khosroshahi, and R Taherzadeh Mousavian. 2013. Microstructural and mechanical properties of Al-4.5 wt% Cu reinforced with alumina nanoparticles by stir casting method. *International Journal of Minerals, Metallurgy, and Materials* 20 (10):978-985.

Zawrah, MF, Hamdia A Zayed, Raghieba A Essawy, Amira H Nassar, and Mohammed A Taha. 2013. Preparation by mechanical alloying, characterization and sintering of Cu–20wt.% Al 2 O 3 nanocomposites. *Materials & Design* 46:485-490.

Zebarjad, Seyed Mojtaba, and SA Sajjadi. 2006. Microstructure evaluation of Al–Al 2 O 3 composite produced by mechanical alloying method. *Materials & design* 27 (8):684-688.

Zhou, Haiping, Lianxi Hu, Hongfei Sun, and Xianjue Chen. 2015. Synthesis of nanocrystalline Mg-based Mg–Ti composite powders by mechanical milling. *Materials Characterization* 106:44-51.